

A SELF-CONSISTENT TURBULENT MODEL FOR SOLAR CORONAL HEATING

J. HEYVAERTS

Université Paris 7 and Observatoire de Paris/DAEC, 92195 Meudon, France

AND

E. R. PRIEST

University of St. Andrews, Solar Theory Group, St. Andrews, KY16 9SS, Scotland, UK

Received 1991 March 26; accepted 1991 October 17

ABSTRACT

The rate of solar coronal heating induced by the slow random motions of the dense photosphere is calculated in the framework of an essentially parameter-free model. This model assumes that these motions maintain the corona in a state of small-scale MHD turbulence. The associated dissipative effects then allow a large-scale stationary state to be established. The solution for the macroscopic coronal flow and the heating flux is first obtained assuming the effective (turbulent) dissipation coefficients to be known. In a second step these coefficients are calculated by the self-consistency argument that they should result from the level of turbulence associated with this very heating flux. For the sake of tractability the derivation is restricted to a two-dimensional situation where boundary flows are translationally symmetric. The resulting value of the heating rate and the predicted level of microturbulent velocity compare satisfactorily with the observational data.

Subject headings: MHD — Sun: corona — turbulence

1. INTRODUCTION

The heating of the solar corona is a long-standing puzzle for solar physicists. When observations (Athay & White 1979; Mein & Schmieder 1981) had shown that the acoustic heating theory (Schatzman 1949; Kuperus, Ionson, & Spicer 1981) could not explain the heating of the corona, the concept of a magnetically heated corona emerged. It explained the observed magnetic structuring (Vaiana & Rosner 1978) and had the potential of accounting for the heating as well. However, the main difficulty with this idea was that the dissipative processes associated with molecular friction are very small in the corona, thus calling for extremely small scales to provide a consistent picture.

A large number of suggestions then blossomed in the literature as to how such a situation could arise: resonant MHD wave processes in magnetic loops of finite length (Wentzel 1979; Ionson 1982; Grossman & Smith 1988; Poedts, Goossens, & Kerner 1990), phase mixing of shear Alfvén waves (Heyvaerts & Priest 1983), triggering of complex reconnection inside magnetic loop structures (Chiuderi 1980), buildup of current concentration by stochastic shuffling of footpoints of coronal field lines (Parker 1983; van Ballegoijen 1986). Most of these processes have been considered independently in other contexts, in the field of laboratory plasma physics, such as, for example, wave resonance phenomena (Hasegawa & Uberoi 1982) or tearing mode turbulence (Strauss 1986).

At the same time it became quite apparent that virtually none of these processes could possibly be found in a laminar regime. Most of them, in any case, even when laminar, involve some sort of cascading process toward smaller scales. This is so for wave resonant processes and phase mixing (see Bondeson 1985) and also for Parker's current concentration buildup process (van Ballegoijen 1986). Needless to say, a laminar evolution is more the exception than the rule because of the large value of the molecular Reynolds numbers involved, and in fact the presence of instabilities has been identified in most

of these processes (Heyvaerts & Priest 1983; Browning & Priest 1984; Chiueh & Zweibel 1987).

This leads to the idea that all these mechanisms share the common property of producing a turbulent state of the coronal medium, the heating being just the end-product of the cascading process (Hollweg, 1984; Heyvaerts & Priest 1983; Tsinganos, Distler, & Rosner 1984; Pettini, Vulpiani, & Nocera 1985; Heyvaerts 1990).

A more detailed description of the evolution of these ideas and of the present situation can be found in the proceedings of the recent IAU Symposium 142 (Heyvaerts 1990; van Ballegoijen 1990).

Thus, turbulence concepts came to be considered as potentially useful tools for the description of coronal heating (Pettini et al. 1985). The present theory of MHD turbulence, which usually addresses isotropic and homogeneous situations, however, has elaborated a number of concepts, such as rugged invariants and selective decay, which, although sometimes not yet rigorously established, prove very useful in assessing the state toward which the turbulent system is going to decline (Taylor 1986; Grappin et al. 1982; Ting, Matthaeus, & Montgomery 1986). This kind of information is useful in identifying the amount of energy available for heating in different magnetic structures. It can be used in conjunction with a phenomenological estimation of the relaxation time to provide a parameterized estimate of the heating rate that results from a balance between stressing and turbulent relaxation of the coronal medium (Heyvaerts & Priest 1984; Browning et al. 1986; Vekstein 1987). Such calculations and similar approaches more or less explicitly involving phenomenologically determined relaxation times or characteristic correlation times (Parker 1983; van Ballegoijen 1986) are useful in pointing to major factors which influence the rate of heating, such as departure from a force-free situation, finiteness of the relaxation time, geometrical factors, ratio of the relaxation to coherence time of the driving motions and so forth.

Still, parameterized theories are incomplete in the sense that they do not unambiguously yield the answer (the rate of heating) only in terms of properties of the driver (the photospheric motions). This is because they lack dynamic considerations.

The possibility of finding the driven state of a dissipative system by use of a variational principle (minimum rate of energy dissipation) is a subject of present study (Montgomery, Phillips, & Theobald 1989) but is not yet well understood enough to be used in the case of a completely turbulent system. By contrast, cascade theories of homogeneous turbulence provide a reasonably satisfactory description of the state of such a driven system, although restricted to the level of its small scales.

It seems then that the missing link for a consistent theory of turbulent heating of a stressed medium, like the solar corona, is the calculation of the macroscopic (large-scale) flow which results from the driving, and which would be consistent with the information on the medium's microstate (small scales) available from existing cascade theories of turbulence.

The aim of this paper is to provide such a consistent calculation in a simplified model of driven motions. Since such a calculation incorporates consideration of the dynamics of the turbulence, it is self-consistent, and a definite parameter-free formula for the rate of heating will result.

The calculation follows the following line of reasoning. It is first assumed that, due to microscale turbulence, the coronal medium is endowed with an effective viscosity and resistivity of unknown values. Generalizations to allow for other kinds of transport coefficients, such as an alpha effect, which are specific to turbulent transport, could have been included but were not, for the sake of simplicity. Then the stationary state of this dissipative medium subject to stresses by boundary motions is calculated, the viscosity and the resistivity being treated as parameters. This solution then gives the energy flux which in a stationary state is fed by the driver (the photosphere) into the dissipative load (the corona). This flux will be dissipated in the corona through a turbulent cascade process leading to its eventual dissipation. Then, for given effective dissipation coefficients the (average) energy dissipation rate per unit mass associated with this cascade is known from the previous macroscopic calculation. But this rate, as is well known, is just the parameter which completely determines the cascade in the inertial range, its level, and ultimately the effective dissipative coefficients themselves. Then we can "bootstrap" this result by requiring that the effective dissipative coefficients which result from this microstate be just those which yielded the previously calculated macroscopic state. This argument thus leads to an equation for the effective dissipative coefficients, the solution of which allows us finally to calculate the actual heating flux.

In the next section, we describe the macroscopic model studied in this paper and calculate the associated macroscopic flow. In § 3, we describe the turbulence model adopted, make explicit the relation between the effective dissipation coefficients and the power provided by the system driving the turbulence, and write the "self-consistency equation" which finally determines them in the present model. In § 4, we particularize to the case where the boundary-driving motions are complex and characterized by a broad spatial Fourier spectrum. The corresponding self-consistency equation is solved in § 5, and the predicted coronal heating rate is derived, numerically evaluated, and discussed. Concluding remarks are made in § 6.

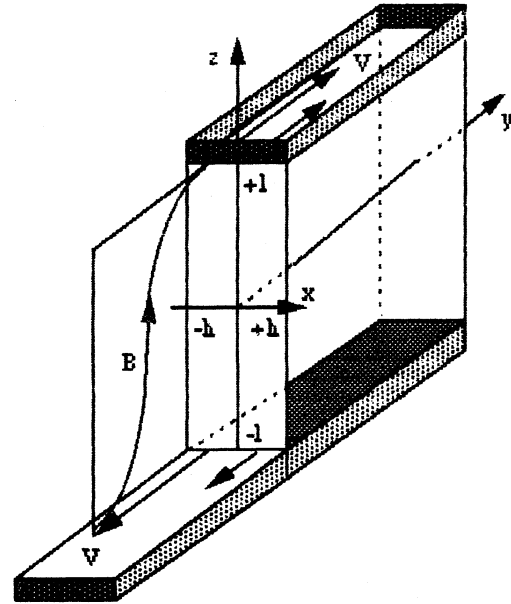


FIG. 1.—The geometry of the flow considered in this paper. The "coronal medium" is the region $-h < x < +h$, $-1 < z < +1$. The upper and lower boundaries at $z = \pm 1$ represent two parts of the photospheric boundary. A magnetic field links the lower to the upper boundary. Motions parallel to the y -axis in the boundaries drive the coronal medium by viscous and Lorentz stresses.

2. THE MACROSCOPIC DISSIPATIVE FLOW

We consider the situation represented in Figure 1. A low-density plasma fills the space of a tube of rectangular cross section. The y -axis, along the tube, is a direction of invariance. In the absence of motions the plasma is permeated by a homogeneous magnetic field in the "vertical" direction, $B_0 \hat{z}$, which meets "horizontal" boundary plates at $z = -1$ and $z = +1$. The latter represent the "photospheric" surface at both ends of a magnetic loop which is here schematized by a translationally invariant structure contained in the region $-1 < z < +1$, $-h < x < +h$, $-\infty < y < +\infty$, which we refer to as "the coronal medium." For the sake of simplicity, the plasma in this medium is assumed to be incompressible. Since the original field is assumed to be homogeneous in $-h < x < +h$, the length h should be regarded as representative of the coherence length of the magnetic field at the base of the corona. Note that we ignore any complications arising from the concentrated nature of the fields in the photosphere, and so B_0 is representative of the average value of the field at the base of the corona rather than in the photosphere itself. Although we shall loosely use the term "photospheric boundaries" when referring to the surfaces at $z = +1$ and -1 , we indeed mean the surface where the "beta" parameter of the plasma becomes of order unity. The length $2l$ should be regarded as representative of the size of loops in their longitudinal direction. The photospheric boundary is the seat of horizontal motions independent of the state of the coronal medium. We assume these motions to be oriented in the y -direction and to be opposite to each other at conjugate points at the lower, $z = -1$, and upper, $z = +1$, boundary, so that

$$v(x, y, 1) = -v(x, y, -1) = V(x)\hat{y}. \quad (1)$$

The profile with x of $V(x)$ is otherwise arbitrary. These boundary motions drive motions and electric currents in the viscous and resistive coronal medium. Let us stress again that the viscosity and resistivity we are referring to are not the molecular ones but originate from the turbulence in the medium, maintained by the energy injection associated with the boundary driving, which, we assume, gives rise to coronal motions which indeed generate turbulence. After some time a permanent regime will be established, which is similar to the well-known plane Couette flow. It is actually a two-dimensional, MHD, version of this classical problem. It is in this stationary state that we are interested. Note that this is at variance with the usual approaches to coronal heating which assume frozen-in-motions. Again the turbulence which is maintained in the corona by the photospheric motions is what makes such a nonfrozen stationary state possible on the large scale. Although the large-scale flow is stationary, a certain amount of energy flux nevertheless flows from the photospheric boundary to the coronal region where it is dissipated.

The usual MHD equations for an incompressible medium govern this flow. Let \mathbf{u} be the velocity field, ρ the mass density, P the pressure, \mathbf{B} the magnetic field, \mathbf{J} the current density, \mathbf{E} the electric field, \mathbf{q} the heat flux vector, $\bar{\sigma}$ the viscous stress tensor, Σ the electrical conductivity, and η_v the dynamic shear viscosity coefficient. These equations can be written, in dimensional form, as

$$\operatorname{div}(\mathbf{u}) = 0, \quad (2)$$

$$\rho \left[\frac{\partial \mathbf{u}}{\partial t} + (\mathbf{u} \cdot \nabla) \mathbf{u} \right] = -\nabla P + \mathbf{J} \times \mathbf{B} - \nabla \times (\eta_v \nabla \times \mathbf{u}), \quad (3)$$

$$\frac{\partial}{\partial t} \left(\frac{1}{2} \rho u^2 + \frac{P}{\gamma - 1} + \frac{B^2}{2\mu_0} \right) + \operatorname{div} \left(\frac{1}{2} \rho u^2 \mathbf{u} + \frac{\gamma}{\gamma - 1} P \mathbf{u} + \mathbf{q} - \mathbf{u} \cdot \bar{\sigma} + \frac{\mathbf{E} \times \mathbf{B}}{\mu_0} \right) = S, \quad (4)$$

$$\partial B / \partial t = \nabla \times (\mathbf{u} \times \mathbf{B}) - \nabla \times (\eta_m \nabla \times \mathbf{B}), \quad (5)$$

$$\mu_0 \mathbf{J} = \operatorname{curl} \mathbf{B}, \quad (6)$$

$$\mathbf{J} = \Sigma (\mathbf{E} + \mathbf{u} \times \mathbf{B}), \quad (7)$$

$$\operatorname{div} \mathbf{B} = 0, \quad (8)$$

$$\sigma_{ij} = \eta_v \left(\frac{\partial v_i}{\partial r_j} + \frac{\partial v_j}{\partial r_i} \right). \quad (9)$$

The right-hand side of the energy equation represents the gains or losses per unit volume and time which are not brought about by kinetic, internal, or magnetic energy transport, such as, radiative cooling or heating. The viscosity, η_v , and resistivity η_m ($= 1/\mu_0 \Sigma$) are meant to be macroscopic manifestations of small-scale turbulence. If the coronal turbulence had kinetic helicity, or if the turbulent magnetic fluctuations had magnetic helicity, further effective transport coefficients would appear in the equations. Although the macroscopic state we are going to find may be endowed with macroscopic helicity, we still assume that in the eventual stationary state the turbulent fluctuations at the boundary do not inject any "microscopic" helicity, kinetic, or magnetic, on the small scale. The global macroscopic magnetic helicity that the system would possess in a stationary state would have been injected by large-scale motions during the nonstationary buildup phase which eventually leads to this stationary state. Of course, in a

stationary state there is no further net macroscopic magnetic helicity injection because the latter does not decay since it suffers an inverse cascade, and then the system could otherwise not be stationary. However, the system being still driven in this regime, we should not expect it to relax completely to a Taylor state either, a deviation from this state being permanently rebuilt (Heyvaerts & Priest 1984; Montgomery 1990). In our previous work (Heyvaerts & Priest 1984), this effect had been schematized by a succession of episodes of deviations from a Taylor state, followed by episodes of relaxation. In the present work the magnetic structure achieved in the stationary state will be calculated more directly. We also assume that the turbulence in the coronal region has zero correlation that is,

$$\int_{-h}^{+h} dx \int_0^L dy \int_{-l}^{+l} dz \langle \mathbf{u} \cdot \mathbf{B} \rangle = 0. \quad (11)$$

In brief, the assumption that no helicity or correlation is injected in the system once the large-scale stationary state is reached allows us to treat its macroscopic motion as an ordinary dissipative flow. The fact that this flow should be (large-scale) time-independent asymptotically is in itself a further assumption which should be acceptable in a range of low enough effective Reynolds and Lundqvist numbers. Montgomery et al. (1989) have shown that the state reached by a dissipative, driven system need not be the simplest one could conceive of. A more detailed exploration of such possibilities in the present context is left for future studies. However, the Reynolds numbers involved, being "effective" ones, are expected to be of order unity, so we do not expect our macroscopically stationary solution to be systematically above instability threshold. But it would certainly be unstable for the molecular Reynolds numbers, and this indeed is why it is maintained in a state of small-scale turbulence.

The equation of energy is the source of our information concerning the heating of the coronal medium. In the absence of mass flow through the boundary ($u_z = 0$ at $z = +1$ and -1), the energy flow toward and from the corona at the lower boundary is, say

$$\mathcal{F}_z(-1) = \hat{z} \cdot (\mathbf{q} - \mathbf{u} \cdot \bar{\sigma} + \mathbf{E} \times \mathbf{B} / \mu_0). \quad (12)$$

Since the corona is much hotter, only the last two terms can make a contribution to its heating, which could actually be negative if the corona were exerting positive work onto the photosphere, but this is not so here and the solution confirms that.

Let us now nondimensionalize the basic equations by choosing suitable reference values. Let

$$c_{A_0}^2 = \frac{B_0^2}{\mu_0 \rho}; \quad v = \frac{\eta_v}{\rho} \frac{1}{lc_{A_0}}; \quad \eta = \frac{\eta_m}{lc_{A_0}}; \quad (13)$$

$1/v$ and $1/\eta$ are effective (turbulent) Reynolds and Lundqvist numbers. We introduce the nondimensional variables τ , \mathbf{a} , \mathbf{v} , \mathbf{b} , \mathbf{j} , \mathbf{e} , and β by the following relations:

$$\begin{aligned} t &= (1/c_{A_0})\tau; & \mathbf{r} &= \mathbf{1a}; & \mathbf{u} &= c_{A_0} \mathbf{v}; \\ \mathbf{B} &= B_0 \mathbf{b}; & \mathbf{J} &= (B_0/\mu_0) \mathbf{j}; \\ \mathbf{E} &= c_{A_0} B_0 \mathbf{e}; & P &= (B_0^2/\mu_0) \beta. \end{aligned} \quad (14)$$

Below, the notation ∇ will mean partial derivative with respect to the dimensionless position vector \mathbf{a} , the components of which will still be denoted by x , y , z . The volume of the

coronal medium considered is now defined by

$$-1 < z < +1; \quad -q < x < +q; \quad -\infty < y < +\infty; \quad (15)$$

where

$$q = h/1 \quad (16)$$

is the aspect ratio of the magnetic coronal configuration considered, that is the ratio of the field gradient scale across a loop to its length. With the previous normalizations, the "heating" flux is

$$\mathcal{F} = B_0^2/\mu_0 c_{A0}(-\mathbf{v} \cdot \bar{\boldsymbol{\sigma}}_1 + \mathbf{e} \times \mathbf{b}) = (B_0^2/\mu_0) c_{A0} \phi, \quad (17)$$

where ϕ is the dimensionless heating flux and $\bar{\boldsymbol{\sigma}}_1$ is the dimensionless stress tensor, the i - j component of which is

$$(\sigma_1)_{ij} = v \left(\frac{\partial v_i}{\partial x_j} + \frac{\partial v_j}{\partial x_i} \right). \quad (18)$$

The other useful dimensionless equations are

$$\partial \mathbf{v} / \partial t + (\mathbf{v} \cdot \nabla) \mathbf{v} = -\nabla \beta + \mathbf{j} \times \mathbf{b} - \nabla \times (\mathbf{v} \nabla \times \mathbf{v}); \quad (19)$$

$$\partial \mathbf{b} / \partial t = \nabla \times (\mathbf{v} \times \mathbf{b}) - \nabla \times (\eta \nabla \times \mathbf{b}); \quad (20)$$

$$\mathbf{j} = \nabla \times \mathbf{b}; \quad (21)$$

$$\text{div } \mathbf{b} = 0; \quad (22)$$

$$\text{div } \mathbf{v} = 0. \quad (23)$$

We now seek a solution independent of y and τ where

$$\mathbf{v} = v(x, z) \hat{\mathbf{y}}; \quad (24)$$

$$\mathbf{b} = b_0 \hat{\mathbf{z}} + b(x, z) \hat{\mathbf{y}}. \quad (25)$$

The value b_0 is constant in space from equation (22) and its value is 1 since B_0 in equation (14) is taken to be the constant value of the vertical component of the field. We also assume η and v to be uniform in space. Then equations (22) and (23) are satisfied by the choice (24)–(25). The x - and z -components of the equation of motion reduce to

$$\nabla(\beta + b^2/2) = 0, \quad (26)$$

which gives a means to calculate the pressure field once the magnetic field is known. The y -component of the equation of motion (19) and the induction equation (20) give

$$b_0 \frac{\partial b}{\partial z} + v \Delta v = 0; \quad (27)$$

$$b_0 \frac{\partial v}{\partial z} + \eta \Delta b = 0. \quad (28)$$

We impose the boundary condition that at $|z| > 1$ the flow is known, and satisfies the frozen-in law. So $v(x, z)$ is a known function at $z = \pm 1$:

$$v(x, 1) = V(x); \quad v(x, -1) = -V(x). \quad (29)$$

Since the flow is viscous $v(x, z)$ should be continuous at the boundaries $z = \pm 1$. From the Faraday equation we find that in a stationary flow $\text{curl } (\mathbf{E}) = 0$, which implies that the tangential component of the electric field is continuous at the interface. Since we assume flux freezing in the dense photosphere, this tangential component is, at the lower interface, say:

$$\mathbf{e}_{\text{rphot}} = -V(x) \hat{\mathbf{y}} \times b_0 \hat{\mathbf{z}} = -V(x) \mathbf{x}, \quad (30)$$

In the neighboring coronal medium, at $z = -1 + \epsilon$, the electric field is given by

$$\mathbf{e} = \eta \mathbf{j} - \mathbf{v} \times \mathbf{b}, \quad (31)$$

which has the tangential component:

$$\mathbf{e}_{\text{tcor}} = -\eta \frac{\partial b}{\partial z} \mathbf{x} - V(x) \mathbf{x}, \quad (32)$$

The continuity of the tangential component of the electric field then demands that equations (30) and (32) be equal which gives rise to the boundary condition, also applicable at the upper boundary for similar reasons:

$$\partial b / \partial z = 0, \quad \text{at } z = \pm 1. \quad (33)$$

We make the further simplifying assumption that the flow is odd in z , which means that

$$v(x, z) = -v(x, -z); \quad (34)$$

$$b(x, z) = +b(x, -z); \quad (35)$$

in compatibility with equations (1) and (29). Given these symmetries the boundary conditions reduce to

$$v(x, z) = V(x) \quad \text{at } z = +1; \quad (36a)$$

$$\partial b / \partial z = 0 \quad \text{at } z = +1; \quad (36b)$$

where, again, $V(x)$ is a known function. Solutions of the equations (27) and (28) can easily be found by expanding the x -dependence in a Fourier series, since the problem happens to be spontaneously linear:

$$v(x, z) = \sum_1^{\infty} v_n^{(1)}(z) \cos \frac{n\pi x}{q} + v_n^{(2)}(z) \sin \frac{n\pi x}{q}, \quad (37a)$$

$$b(x, z) = \sum_1^{\infty} b_n^{(1)}(z) \cos \frac{n\pi x}{q} + b_n^{(2)}(z) \sin \frac{n\pi x}{q}. \quad (37b)$$

We substitute these in equations (27) and (28), keeping in mind that b_0 is actually unity. The unknown pairs of functions $(v_n^{(1)}, b_n^{(1)})$ and $(v_n^{(2)}, b_n^{(2)})$ separately satisfy the same system:

$$\frac{db_n^{(i)}}{dz} + v \left(\frac{d^2 v_n^{(i)}}{dz^2} - \frac{n^2 \pi^2}{q^2} v_n^{(i)} \right) = 0; \quad (38a)$$

$$\frac{dv_n^{(i)}}{dz} + \eta \left(\frac{d^2 b_n^{(i)}}{dz^2} - \frac{n^2 \pi^2}{q^2} b_n^{(i)} \right) = 0; \quad (38b)$$

where the superscript (i) means (1) or (2). The elimination of $b_n^{(i)}$ gives for $v_n^{(i)}$ the equation:

$$\eta v \frac{d^4 v_n^{(i)}}{dz^4} - \left(1 + 2\eta v \frac{n^2 \pi^2}{q^2} \right) \frac{d^2 v_n^{(i)}}{dz^2} + \eta v \frac{n^4 \pi^4}{q^4} v_n^{(i)} = 0, \quad (39)$$

which is linear and can easily be solved by introducing the following variables and operators:

$$\sqrt{\eta v} = H; \quad \lambda_n = \sqrt{\eta v} \frac{n\pi}{q}; \quad \xi = \frac{z}{\sqrt{\eta v}};$$

$$D = \frac{d}{d\xi} = \sqrt{\eta v} \frac{d}{dz}; \quad (40)$$

in terms of which it can be written as

$$D^4 v_n^{(i)} - (1 + 2\lambda_n^2) D^2 v_n^{(i)} + \lambda_n^4 v_n^{(i)} = 0. \quad (41)$$

The solution of equation (41) is a linear combination of exponentials, $\exp(\sigma_i \xi)$, the four characteristic exponents σ_i being the solutions of the equation

$$\sigma^4 - (1 + 2\lambda_n^2)\sigma^2 + \lambda_n^4 = 0 \quad \text{or} \quad (\sigma^2 - \lambda_n^2)^2 = \sigma^2, \quad (42)$$

which are

$$\sigma_i = \pm \sigma_{\pm} = \pm \frac{1}{2}(\sqrt{1 + 4\lambda_n^2} \pm 1), \quad (43)$$

Note that the two signs of the alternatives (\pm) are independent of each other. Making some use of the relations between the roots of equation (42) it is easy to find the solutions of (38a)–(38b) which satisfy the boundary conditions (36a)–(36b), which translate as follows for the Fourier coefficients $v_n^{(i)}$ and $b_n^{(i)}$:

$$v_n^{(i)}(\xi) = V_n^{(i)} \quad \text{at} \quad \xi = 1/H, \quad (44a)$$

$$\frac{d^2}{dz^2} v_n^{(i)} = \lambda_n^{(2)} v_n^{(i)} \quad \text{at} \quad \xi = 1/H, \quad (44b)$$

where $V_n^{(i)}$ is either $v_n^{(1)}$ (1) or $v_n^{(2)}$ (1), that is, one of the Fourier coefficients, as defined in equation (37a), of the function $V(x)$. This gives the following result applicable separately to the sin and cos coefficients:

$$v_n^{(i)}(z) = \frac{\lambda_n^2 V_n^{(i)}}{\sqrt{1 + 4\lambda_n^2}} \left\{ \frac{\sinh[\sigma_-(z/H)]}{\sigma_- \sinh[(\sigma_-/H)]} + \frac{\sinh[\sigma_+(z/H)]}{\sigma_+ \sinh[(\sigma_+/H)]} \right\}; \quad (45a)$$

$$b_n^{(i)}(z) = \frac{v}{H} \frac{\lambda_n^2 V_n^{(i)}}{\sqrt{1 + 4\lambda_n^2}} \left\{ \frac{\cosh[\sigma_-(z/H)]}{\sigma_- \sinh[(\sigma_-/H)]} - \frac{\cosh[\sigma_+(z/H)]}{\sigma_+ \sinh[(\sigma_+/H)]} \right\}. \quad (45b)$$

For small dissipative coefficients η and v , $H \rightarrow 0$ and $\lambda_n \rightarrow 0$ at given n . Then $\sigma_+ \rightarrow 1$, and $\sigma_- \rightarrow \lambda_n^2$. The function $v_n^{(i)}(z)$ approaches a linear profile and the function $b_n^{(i)}(z)$ approaches a constant. Both exhibit a small boundary layer near $z = \pm 1$. However, in the present situation, the effective dissipative coefficients need not be small, and the full expression (45a)–(45b) must be used. From this solution we calculate the heating flux defined at equation (17), the dimensionless z -component of which is given by

$$\phi_z = \hat{z} \cdot (-\mathbf{v} \cdot \bar{\sigma}_1 + \mathbf{e} \times \mathbf{b}). \quad (46)$$

This flux consists of a viscous and a Poynting part, which are the first and second terms on the right-hand side of equation (46), respectively. The Poynting part may be conveniently expressed by noting that, since the tangential component of the electric field is continuous at the boundary, and since flux freezing applies in the photospheric medium:

$$\hat{z} \times \mathbf{e} = -[\hat{z} \times (\mathbf{v} \times \hat{z})] = -V\hat{y}. \quad (47)$$

As a result, the Poynting contribution to equation (46) is

$$\phi_{z\text{Poynt}} = -vb, \quad (48a)$$

while the viscous contribution is

$$\phi_{z\text{visc}} = -v \frac{\partial v}{\partial z}. \quad (48b)$$

Both terms on the right-hand side of (48a)–(48b) are negative because, at the upper boundary, presently considered, the normal entering the coronal medium is $-\hat{z}$. A similar contribu-

tion, with opposite sign, is obtained from the lower boundary. It is convenient to calculate the average flux entering through the upper boundary, defined as

$$|\langle \phi_z \rangle| = \left| \frac{1}{2q} \int_{-q}^{+q} dx \phi_z \right|. \quad (49)$$

Substituting for $v(x, z)$ and $b(x, z)$ in the solution (45a)–(45b), the following results are obtained:

$$|\langle \phi_{z\text{Poynt}} \rangle| = \sum_1^{\infty} \frac{V_n^2}{2\eta} \times \frac{(H/\sqrt{1 + 4\lambda_n^2}) \sinh[(\sqrt{1 + 4\lambda_n^2}/H)] + H \sinh(1/H)}{\cosh(\sqrt{1 + 4\lambda_n^2}/H) - \cosh(1/H)}; \quad (50a)$$

$$|\langle \phi_{z\text{visc}} \rangle| = \sum_1^{\infty} \frac{V_n^2}{2\eta} 2\lambda_n^2 \frac{(H/\sqrt{1 + 4\lambda_n^2}) \sinh[(\sqrt{1 + 4\lambda_n^2}/H)]}{\cosh[(\sqrt{1 + 4\lambda_n^2}/H)] - \cosh(1/H)}. \quad (50b)$$

We defined the dimensionless power spectrum of the boundary velocity motions by

$$V_n^2 = V_n^{(1)2} + V_n^{(2)2}. \quad (51)$$

The net average heating flux entering the coronal medium through the upper boundary is the sum of equations (50a) and (50b). The contribution from the lower boundary adds another term of the same value. Then the average of the dimensionless heating flux through both boundaries, F , is

$$F = \sum_1^{\infty} \frac{V_n^2}{\eta} \frac{H \sinh(1/H)}{\cosh[(\sqrt{1 + 4\lambda_n^2}/H)] - \cosh(1/H)} + \frac{V_n^2 (1 + 2\lambda_n^2)(H/\sqrt{1 + 4\lambda_n^2}) \sinh[(\sqrt{1 + 4\lambda_n^2}/H)]}{\eta \cosh[(\sqrt{1 + 4\lambda_n^2}/H)] - \cosh(1/H)} \quad (52)$$

3. THE STATE OF TURBULENCE AND THE EFFECTIVE DISSIPATION

In the framework of our present assumptions (no helicity or correlation injection) the three-dimensional turbulence which is supposed to exist in the medium has direct cascades of kinetic and magnetic energy toward the small scales which bring it to dissipation. Since there is an ordered magnetic field in the medium, which we shall assume has an energy density larger than that of the turbulence, the dynamics of the latter at small scales is dominated by the ‘‘Alfvén effect’’ (Kraichnan 1965). In this situation the turbulent eddies are mainly destroyed by the (inhomogeneous) propagation effects associated with Alfvén waves in a time of order $1/\Delta c_A(1)$, where 1 is the eddy size and $\Delta c_A(1)$ is the detuning of the Alfvén velocity over a distance 1, while in the usual Kolmogoroff situation the lifetime of an eddy is $1/v(1)$, where $v(1)$ is now the characteristic velocity associated with an eddy of that size. The Kraichnan regime leads to a spectrum proportional to $k^{-3/2}$. Closure approximations (Pouquet, Frisch, & Léorat 1976) give in many respects a satisfactory description of these turbulent regimes, which compare favorably with direct numerical simulations, although some important aspects, such as intermittency, are lost. Closure models, such as the eddy-damped quasi-normal Markovian approximation (EDQNM), provide enough of the macroscopic information we are seeking, we believe. Pouquet

et al. analyzed isotropic, homogeneous MHD turbulence in the framework of this closure theory, which leads to a set of integro-differential equations for the spectral energy and helicity densities, involving an “eddy-damping relaxation rate” which captures the essence of the approximation made to the actual dynamics. We assume here that this relaxation rate is, in fact, dominated by the Alfvén effect (eq. [56] below) associated with the large-scale field. In fact, we adopted an expression for this rate involving such a field, as Kraichnan initially introduced it, rather than the rms field at scales larger than $1/k$, as Pouquet et al. had to do, since, consistently with their isotropy assumption, they did not assume such an ordered field to be present in their system. Note that in our case where an ordered field is present, the turbulence would, in general, be anisotropic. Nevertheless, effective dissipation coefficients have been evaluated below ignoring this complicating aspect. We comment later on the consequences of this simplification.

In the regime where there is no helicity injection and the Alfvén effect dominates, there is equipartition at small scales between magnetic and kinetic energy of the fluctuations (Kraichnan 1965). A simplification of the EDQNM equations can be obtained when the nonlocal terms, i.e., those which are associated with scales much larger or much smaller than the scale $1/k$ of interest, are expanded in the scale ratio. This gives rise to two kinds of terms, those involving the effect of larger scales, which actually vanish in our case, due to equipartition and the fact that this turbulence is deprived of helicity, and those involving the effect of smaller scales, which give rise to “effective dissipation.” We assume that the latter terms dominate the dynamics of the larger scales over the so-called local interactions, i.e., terms which involve the interaction of scales of comparable size. In fact, we assume in this paper that, to describe the plasma dynamics on the larger scales, it is sufficient to take into account only these effective dissipation effects. These effects of the small scales on large-scale dynamics appear, in the equation of evolution of the spectral kinetic energy $[E_v(k)]$ and magnetic energy $[E_m(k)]$, as terms similar to viscosities, namely (Pouquet et al. 1976),

$$\frac{\partial}{\partial t} [E_v(k)]_{\text{nss}} = -2\left(\frac{2}{3}v_k^V + v_k^M + v_k^R\right)k^2 E_v(k); \quad (53)$$

$$\frac{\partial}{\partial t} [E_m(k)]_{\text{nss}} = -2v_k^V k^2 E_m(k); \quad (54)$$

where “nss” means “nonlocal small scales.” The various v_k^x s which appear in these formulae are contributions to the effective viscosity and magnetic diffusivity, respectively. When there is equipartition, $v_k^R = 0$, and $v_k^M = v_k^V$, so that the effective viscosity and magnetic diffusivity are

$$\eta_v = \frac{7}{5}\rho v_k^V; \quad \eta_m = v_k^V. \quad (55)$$

Note that these coefficients should be regarded as scale-dependent, but in the following we shall also disregard this dependence and evaluate the effective viscosity and resistivity at the injection scale. The coefficient v_k^V is expressed in terms of an eddy-damping rate at small scales, μ_p , which, when the Alfvén effect dominates, reduces, for a wavenumber p , to

$$\mu_p = \frac{p c_{A0}}{\sqrt{3}}. \quad (56)$$

Then

$$v_k^V = \frac{2}{3} \int_k^\infty \frac{\sqrt{3}}{2p c_{A0}} E(p) dp. \quad (57)$$

Here $E(p)$ is the common value of the kinetic and magnetic spectrum. Note that this expression, which Pouquet et al. obtained, involves angular averages which have been carried out assuming isotropy. One effect of the turbulence spectrum being actually anisotropic would be to change the numerical coefficient in this expression from $\frac{2}{3}$ to some other value, $E(p)$ now being interpreted as an angle average of the turbulence spectrum. Since the turbulence, though in reality not totally isotropic, is not likely to reduce exactly to two-dimensional motions either, we do not expect more fundamental changes, such as the appearance of inverse cascades, with respect to the completely isotropic case. In the Kraichnan regime, the energy spectrum is given by

$$E(p) = C \sqrt{\epsilon c_{A0}} p^{-3/2}, \quad (58)$$

where ϵ is the energy transfer rate, that is, the energy absorbed per unit time and per unit mass as a result of the cascade, and C is a dimensionless constant of order unity which is not precisely known. In the nonmagnetic situation, a similar constant appears, which can be chosen on the basis of the argument that it should reproduce the experimentally known value of the Kolmogoroff constant. No such fine tuning is, to our knowledge, possible for the strongly magnetized situation, where nothing like a Kolmogoroff constant for the Kraichnan spectrum has been measured. So C in equation (58) should be regarded as a parameter. Adopting the normalization of the Alfvén eddy damping time of Pouquet et al. (1976) yields, according to their numerical results, a spectrum almost exactly equal to $k^{-3/2}$, for an energy transfer rate equal to 0.5 and an injection situated at $k = 1$ in their units. Taking into account the part of the spectrum at $k < 1$ too, their results indicate a value of C very near unity, namely, $C = 0.9$. From equations (55a)–(55b), (57), and (58) we obtain the following expressions for the effective dissipation coefficients:

$$\eta_m = \frac{2C\sqrt{3}}{9} \sqrt{\frac{\epsilon}{c_{A0}}} k_{\text{min}}^{-3/2}; \quad (59a)$$

$$\eta_v = \rho \frac{7}{5} \eta_m; \quad (59b)$$

where k_{min} is the smallest wavenumber excited by the injection. Since we expect the turbulence to be generated by resistive instabilities occurring in the stressed structure, the flows produced by these primary instabilities could have cross-field characteristic scales comparable to the field gradient scales. Then, in the present model the injection scale would be of the order of

$$k_{\text{min}} = 2\pi/2h = \pi/h. \quad (60)$$

Strictly speaking, the situation then does not have the injection scale smaller than the gradient scale, so that, rigorously, it should not be described as homogeneous turbulence, and the dissipative terms would in reality become some spatially nonlocal operators instead of being representable by the usual local coefficients. For the sake of simplicity, however, we still retain the homogeneous assumption and finally obtain the following expressions for these turbulent viscosity and resistivity coefficients:

$$\eta_m = \frac{2C\sqrt{3}}{9} \sqrt{\frac{\epsilon}{c_{A0}}} \left(\frac{h}{\pi}\right)^{3/2}; \quad (61a)$$

$$\frac{\eta_v}{\rho} = \frac{14}{45} C\sqrt{3} \sqrt{\frac{\epsilon}{c_{A0}}} \left(\frac{h}{\pi}\right)^{3/2}. \quad (61b)$$

The model certainly gives a rather sharp definition of this "injection scale" which in the solar reality is less precise. Since also C , in equation (58), is not perfectly well known, and because of the various simplifications which have been made with respect to other aspects of solar reality (regarding isotropy and homogeneity of the coronal turbulence) the quantitative character of our results will necessarily be limited.

The power fed per unit mass into heat by the turbulent transfer of energy has an average value over the coronal region which is, of course, related to the energy flux which enters the corona, and which we calculated in § 2. Indeed, if F is the dimensionless heating flux through both boundaries, the power transmitted to a part of length L in the y -direction of the coronal region is

$$Q = 2hL(B_0^2/\mu_0)c_{A_0}F, \quad (62)$$

while the power which goes into heating in the same region as a result of turbulence dissipation is

$$Q' = 2h2lL\rho\epsilon. \quad (63)$$

When a stationary state is reached, Q' equals Q , and, as a consequence, ϵ is given by just

$$\epsilon = (c_{A_0}^3/2l)F. \quad (64)$$

We are now in a position to relate the dimensionless effective diffusivities, which are given as a function of ϵ by the theory of turbulent cascades (eqs.[61a]–[61b]) to the flux driven by the boundary stresses into the coronal medium. Using equation (13) and relation (64) in equations (61a)–(61b), we obtain these dimensionless diffusivities as a function of F , namely:

$$\eta = \frac{C\sqrt{6}}{9\pi^{3/2}} q^{3/2} F^{1/2}, \quad (65a)$$

$$v = \frac{7C\sqrt{6}}{45\pi^{3/2}} q^{3/2} F^{1/2} = \frac{7}{5} \eta; \quad (65b)$$

where q is the aspect ratio defined at equation (16). Equation (65a) can be rewritten as an expression giving the flux F in terms of the effective magnetic diffusivity, η , or of the effective viscosity, v :

$$F = \frac{27\pi^3}{2C^2} \frac{\eta^2}{q^3} = \frac{675\pi^3}{98C^2} \frac{v^2}{q^3}. \quad (66)$$

This equation summarizes our previous analysis of the micro-scale physics of the effective dissipative coefficients, taking into account the fact that the energy budget of the corona is stationary. Now, the dimensionless flux, F , is also expressed by the equation (52), which concluded the macroscale analysis of the energy injection in the system. Equating equations (52) and (66) we obtain an equation which determines the dimensionless eddy viscosity, v :

$$\frac{3375\pi^3}{686C^2} \frac{v^2}{q^3} = \sum_1^\infty \frac{V_n^2}{v} \frac{H \sin(1/H)}{\cosh[(\sqrt{1+4\lambda_n^2})/H] - \cosh(1/H)} + \frac{V_n^2 (1+2\lambda_n^2)(H/\sqrt{1+4\lambda_n^2}) \sinh[(\sqrt{1+4\lambda_n^2})/H]}{\gamma \cosh[(\sqrt{1+4\lambda_n^2})/H] - \cosh(1/H)}. \quad (67)$$

In this equation λ_n and H are still functions of v , which are

given by (see eqs. [40] and [65b]):

$$H = \sqrt{\frac{5}{7}} v; \quad \lambda_n = \sqrt{\frac{5}{7}} n \frac{\pi v}{q}. \quad (68)$$

Equation (67), which will allow us to calculate the effective viscosity, is the basic equation of this paper. Once solved for v as a function of the parameters of the model, the V_n 's and the aspect ratio q , the average heating flux will be completely determined through equation (66).

4. EQUATION FOR THE EFFECTIVE VISCOSITY IN THE BROAD SPECTRUM LIMIT

Let us introduce the following variables, in terms of which equation (67) will be more conveniently expressed:

$$x = \frac{1}{H} = \sqrt{7/5} \frac{1}{v}; \quad \alpha_n = \frac{2n\pi}{q} = 2\lambda_n x; \\ \Lambda_n = \sqrt{5/7} \frac{98C^2}{675\pi^3} V_n^2 q^3. \quad (69)$$

Then equation (67) takes the form:

$$1 = \sum_1^\infty \Lambda_n x \times \frac{[x^2 + (\alpha_n^2/2)][\sinh(\sqrt{x^2 + \alpha_n^2})/(\sqrt{x^2 + \alpha_n^2})] + x \sinh x}{\cosh(\sqrt{x^2 + \alpha_n^2}) - \cosh x}. \quad (70)$$

It is relatively easy to solve this equation in the case when the boundary motion consists of a single Fourier mode. Although instructive, this case does not correspond closely enough to the solar reality, where the spatial Fourier spectrum of the velocity is broad. The spectrum of the granular velocity has indeed been shown by Roudier & Müller (1987) to be a turbulent continuous spectrum. Later the same authors and partners measured this surface velocity spectrum to scale approximately as $k^{-5/3}$ in the granular range down to subarcsecond scales (Malherbe et al. 1987; Roudier et al. 1990). Since the heating is expected to be dominated by large wavenumber contributions, only that part of the spectrum is of interest, and not the longer wavelength part, which is observed to have a different slope. This gives for the velocity power spectrum of boundary motions:

$$v^2(k)dk = \frac{2}{3} k_{\min}^{2/3} \bar{v}^2 k^{-5/3} dk, \quad (71)$$

where k_{\min} is given by equation (60). The spectrum (71) is related to the discrete and dimensionless spectrum of our model, V_n , defined by equations (36a), (37a), and (51) in the sense that both represent the fluctuations of velocity at the photospheric boundary, although the second is not regarded as random. The link can be made by identifying the expressions of the rms velocity which both of them give, the average procedure in the case of the discrete spectrum being as defined by equation (49). This gives in the model's formulation:

$$\langle v^2 \rangle = c_{A_0}^2 \sum_1^\infty (1/2) V_n^2, \quad (72)$$

where, again, c_{A_0} is the coronal Alfvén velocity. Similarly the

continuous representation (71) gives

$$\langle v^2 \rangle = \int_{k_{\min}}^{\infty} v^2(k) dk = \bar{v}^2. \quad (73)$$

The harmonic number n and the wavenumber k are related by the fact that the length $2h$ is the wavelength which corresponds to the fundamental, $n = 1$. Then

$$k = n\pi/h = (n\pi/q)(1/l). \quad (74)$$

Converting the sum in equation (72) into an integral and using equation (71) shows that

$$v^2(k) = (c_{A_0}^2/2)(h/\pi)V_n^2. \quad (75)$$

Then for the granulation spectrum

$$V_n^2 = 4/3(\bar{v}^2/c_{A_0}^2)n^{-5/3}. \quad (76)$$

In reality, the turbulence spectrum (71) does not extend to $k = \infty$, but up to a dissipation wavenumber, k_{diss} , given by

$$k_{\text{diss}} = k_{\min} R_{\text{phot}}^{3/4}, \quad (77)$$

where R_{phot} is the photospheric Reynolds number. The typical photospheric velocity at a scale λ , $v(\lambda)$, is obtained from equation (71) by

$$v^2(\lambda) = \int_{2\pi/\lambda}^{\infty} v^2(k) dk = \frac{\bar{v}^2}{(2\pi)^{2/3}} (\lambda k_{\min})^{2/3}, \quad (78)$$

and the eddy turnover time, which for a Kolmogoroff type of turbulence in the photosphere will be the coherence time of boundary motions at this scale, is

$$t(\lambda) = \frac{\lambda}{v(\lambda)} = \frac{\lambda}{\bar{v}} \left(\frac{2\pi}{\lambda k_{\min}} \right)^{2/3}. \quad (79)$$

Since our model considers boundary motions as steady, it is, in its present form, only applicable to those boundary motions for which the coherence time $t(\lambda)$ is longer than the Alfvén transit time, t_A :

$$t_A = 1/c_{A_0}. \quad (80)$$

Hence the wavenumber of the horizontal motions for which the present analysis is valid is limited by the condition $t_A < t(\lambda)$, which translates for the wavenumber $k = 2\pi/\lambda$ into the inequality:

$$k < k_A, \quad (81)$$

where k_A is defined by

$$k_A = (\pi/h)(2qc_{A_0}/\bar{v})^{3/2}. \quad (82)$$

Numerically the length $\lambda_A = 2\pi/k_A$ is ~ 1000 times smaller than h , which is of the order of a megameter, and is much larger indeed than the dissipation length, $2\pi/k_{\text{diss}}$, which is of the order of centimeters. Our analysis should then include in the summation on harmonic numbers in equation (70) only those n 's for which inequality (81) is valid, which means (eq. [74]):

$$n < N_A = (2qc_{A_0}/\bar{v})^{3/2}. \quad (83)$$

This does not mean that the boundary motions of smaller scales do not contribute to the coronal heating, but they can do so only by generating wave motions in the corona which would dissipate by an appropriate mechanism, not considered in this paper, like, for example, phase mixing (Heyvaerts & Priest 1983).

In practice, since the upper bound (83) is very large because c_{A_0} is much larger than \bar{v} , the discrete summation, in equation (70) can be converted to an integral. Let

$$K = n\pi/q \quad (84)$$

be treated as a continuous variable, and write (see eq. [69]):

$$\Lambda_n = \Lambda(K); \quad \alpha_n = 2K.$$

Then equation (70) can be approximately written, in the harmonic rich limit, as

$$1 = \frac{q}{\pi} \int_{K_m}^{K_M} dK x \Lambda(K) \times \frac{(x^2 + 2K^2/\sqrt{x^2 + 4K^2}) \sinh(\sqrt{x^2 + 4K^2}) + x \sinh x}{\cosh(\sqrt{x^2 + 4K^2}) - \cosh x}, \quad (85)$$

where

$$K_m = \pi/q; \quad K_M = N_A K_m.$$

The function $\Lambda(K)$, (eq. [69]), is directly proportional to the excitation spectrum. For the Kolmogoroff distribution (76) we have

$$\Lambda(K) = \sqrt{5/7} \frac{392}{2025} c^2 \left(\frac{\bar{v}^2}{c_{A_0}^2} \right) \left(\frac{q}{\pi} \right)^{4/3} K^{-5/3} \\ \Lambda(K) = \Lambda_0 K^{-5/3} \quad (86)$$

The latter relation defines the factor Λ_0 . The function

$$\psi(x, K) = \frac{[(x^2 + 2K^2)/\sqrt{x^2 + 4K^2}] \sinh(\sqrt{x^2 + 4K^2}) + x \sinh x}{\cosh(\sqrt{x^2 + 4K^2}) - \cosh x} \quad (87)$$

essentially describes the efficiency of each boundary mode to inject flux into the coronal medium, where it will be dissipated.

5. HEATING RATE OF THE CORONAL MEDIUM

Since the aspect ratio, q , is of the order of 10^{-1} , and is large anyway, K_m is a large number and at least those hyperbolic functions which have argument $(x^2 + 4K^2)^{1/2}$ can be approximated by exponentials. If x itself is not large, $x \sinh x$ and $\cosh x$ are negligible as compared to the accompanying terms in the numerator and denominator of equation (87), as is, in this case, $\exp x$ too. Then in all cases it is good enough to approximate all the hyperbolic functions by exponentials. So doing, equation (87) reduces to

$$\psi(x, K) = \frac{[(x^2 + 2K^2)/\sqrt{x^2 + 4K^2}] \exp(\sqrt{x^2 + 4K^2} - x) + x}{\exp(\sqrt{x^2 + 4K^2} - x) - 1}. \quad (88)$$

This function has several different behaviors according to whether

$$(a) \quad x \ll K \quad \leftrightarrow \quad K \gg x; \quad (89a)$$

$$(b) \quad K \ll x \ll K^2 \quad \leftrightarrow \quad \sqrt{x} \ll K \ll x; \quad (89b)$$

$$(c) \quad x \gg K^2 \quad \leftrightarrow \quad K \ll \sqrt{x}. \quad (89c)$$

In the ranges a and b , the argument of the exponential in equation (88) is large, whereas it is small in the range c . In

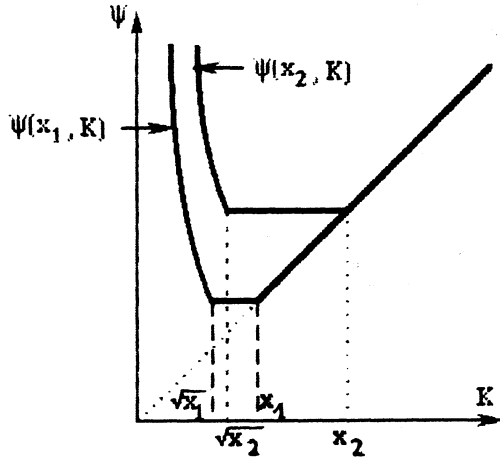


FIG. 2.—A representation of the approximation (90a), (90b), and (90c) to the function $\psi(x, K)$ defined by eq. (87). The variable is K , and x is a parameter. Two such curves are represented for two different values of x , x_1 and x_2 , the former being smaller than the latter.

ranges b and c the term proportional to x^2 dominates in the factor $(x^2 + 2K^2)$ which, coming back to equation (50a) and (50b), means that the Poynting flux dominates the energy entering the corona for these scales, while in the range a the viscous flux dominates. In the different ranges defined by equations (89a), (89b), and (89c), $\psi(x, K)$ can be approximated by

$$\psi(x, K) = K \quad \text{in (a)}; \quad (90a)$$

$$\psi(x, K) = x \quad \text{in (b)}; \quad (90b)$$

$$\psi(x, K) = x^2/K^2 \quad \text{in (c)}. \quad (90c)$$

At a given K , $\psi(x, K)$ is an increasing function of x , and so is the integral at the right-hand side of equation (85). At a given x , $\psi(x, K)$ is the function of K which is represented in Figure 2, for two different values of x . To calculate finally the right-hand side of equation (85), the expressions (90a), (90b), and (90c) should be substituted for $\psi(x, K)$, as defined by equation (87), into it, and the boundaries of the various regimes (89a), (89b), and (89c) $x^{1/2}$ and x , should be placed with respect to the integration limits K_m and K_M . The details of this placement, and the calculation of the actual right-hand side of equation (85) are presented in Appendix A.

It is worth noting that the function on the right-hand side of equation (85), considered as a function of x , starts at a vanishing value at $x = 0$, and increases monotonically to infinity since, according to equation (90c), it behaves as x^3 for large x (see Appendix A). Therefore equation (85) has one and only one solution, whatever the excitation spectrum $\Lambda(K)$. For a Kolmogoroff one (eq. [86]) and an upper limit of the DC excitation spectrum, K_M , larger than K_m^2 , equation (85) breaks down into the following forms on the various subintervals indicated (see Appendix A):

$$x < K_m,$$

$$\frac{K_m}{3\Lambda_0} = x(K_m^{1/3} - K_m^{1/3}); \quad (91a)$$

$$K_m < x < K_M^2,$$

$$\frac{K_m}{3\Lambda_0} = \frac{x^2}{2} K_m^{-2/3} - \frac{3}{2} x^{4/3} + x K_m^{1/3}; \quad (91b)$$

$$K_m^2 < x < K_M,$$

$$\frac{K_m}{3\Lambda_0} = \frac{x^3}{8} K_m^{-8/3} + \frac{3}{8} x^{5/3} - \frac{3}{2} x^{4/3} + x K_m^{1/3}; \quad (91c)$$

$$K_M < x < K_M^2,$$

$$\frac{K_m}{3\Lambda_0} = \frac{x^3}{8} K_m^{-8/3} + \frac{3}{8} x^{5/3} - \frac{x^2}{2} K_M^{-2/3}; \quad (91d)$$

$$K_M^2 < x,$$

$$\frac{K_m}{3\Lambda_0} = \frac{x^3}{8} (K_m^{-8/3} - K_M^{-8/3}). \quad (91e)$$

This composite equation should be solved numerically for appropriate parameters of the photospheric and coronal plasmas. Let us adopt the following representative values:

$$h = Q \times 1000 \text{ km}, \quad l = 10,000 \text{ km}, \quad v = w \text{ km s}^{-1}, \quad (92)$$

$$B = M \times 100 \text{ G}, \quad n = D \times 10^{10} \text{ cm}^{-3},$$

where n is the coronal density. With these values we obtain

$$c_{A0} = 2178MD^{-1/2} \text{ km s}^{-1}; \quad (93a)$$

$$q = 0.1Q; \quad (93b)$$

$$K_m = 31.4Q^{-1}; \quad (93c)$$

$$K_M = 2.86 \times 10^5 Q^{1/2} M^{3/2} w^{-3/2} D^{-3/4}; \quad (93d)$$

$$3\Lambda_0/K_m = 3.32 \times 10^{-11} C^2 Q^{7/3} w^2 M^{-2} D. \quad (93e)$$

With these parameters we can show that the solution of equation (91) is in the domains (3) or (4) (see eq. [93c] or [93d]). We let

$$x = K_m^2 X. \quad (94)$$

Equation (91c) then becomes

$$1 = 4.05 \times 10^{-7} C^2 Q^{-1} w^2 M^{-2} D (X^3 + 3X^{5/3} - 1.21Q^{2/3} X^{4/3} + 5.376Q^{3/2} M^{1/2} w^{-1/2} D^{-1/4} X), \quad (95)$$

and equation (91d) becomes

$$1 = 4.05 \times 10^{-7} C^2 Q^{-1} w^2 M^{-2} D \times (X^3 + 3X^{5/3} - 9.18 \times 10^{-3} Q^{-1} M^{-1} w D^{1/2} X^2). \quad (96)$$

Equation (95) is valid for $1 < X < K_M/K_m^2$ and equation (96) for $K_M/K_m^2 < X < K_M^2/K_m^2$. Substituting $X = 1$ in equation (95) shows its right-hand side to be much less than unity, whereas substituting $X = K_M^2/K_m^2$ in equation (96) shows its right-hand side to be much larger than unity. These inequalities are strong enough to be valid for any reasonable set of parameters Q , w , M , D . Under these conditions, since the value of X which solves equations (95) or (96) is not near unity either, the X^3 term dominates in both forms of the equation, and the solution is, to a good approximation

$$X = (4.05 \times 10^{-7} C^2 Q^{-1} w^2 M^{-2} D)^{-1/3} = 135C^{-2/3} Q^{1/3} w^{-2/3} M^{2/3} D^{-1/3}, \quad (97)$$

which using equation (94) gives

$$x = 1.33 \times 10^5 C^{-2/3} Q^{-5/3} w^{-2/3} M^{2/3} D^{-1/3}. \quad (98)$$

From this we obtain the dimensionless heating flux per unit

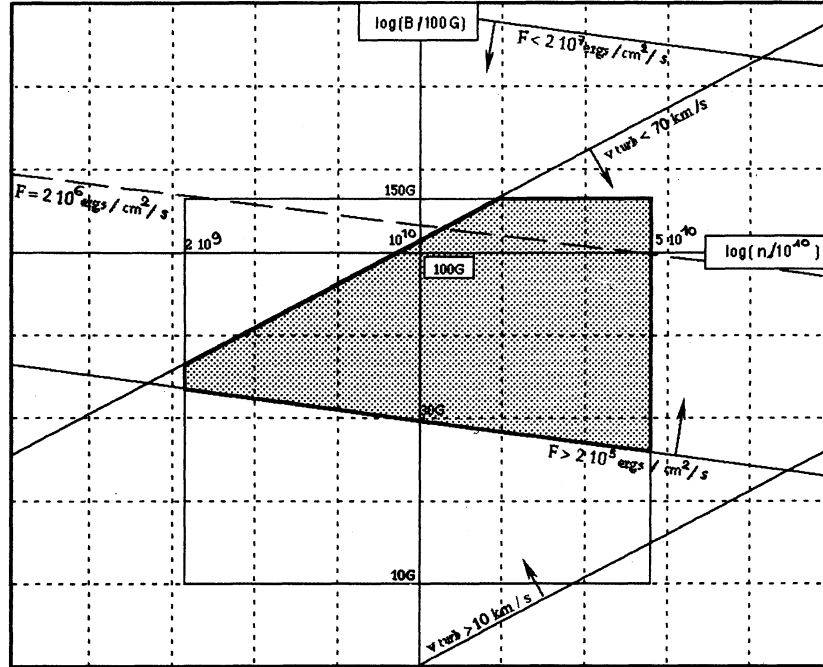


FIG. 3.—A representation of the parameter space (density and magnetic field) where our theory gives results consistent with the observational data. The constraints imposed are that for a granular velocity of 1 km s^{-1} and an aspect ratio $q = 0.1$, the following conditions be satisfied: (1) equation (104) gives a flux between 2×10^5 and $2 \times 10^7 \text{ ergs cm}^{-2} \text{ s}^{-1}$. (2) equation (105) gives a turbulent velocity between 10 and 70 km s^{-1} . (3) The coronal density be between $2 \times 10^9 \text{ cm}^{-3}$ and $5 \times 10^{10} \text{ cm}^{-3}$. (4) The magnetic field be between 10 and 150 G. The various full straight lines in the figure represent these various limits. The shaded area is the region of parameter space that satisfies all four conditions. The dotted line is the locus of conditions giving rise to a heating of $2 \times 10^6 \text{ ergs cm}^{-2} \text{ s}^{-1}$.

photospheric area, F_1 , which is half of equation (66). Using equation (69) we find

$$F_1 = \frac{F}{2} = \left(\frac{1}{2}\right) \frac{675\pi^3}{98C^2} \frac{1}{q^3} \frac{7}{5x^2} \\ = 8.42 \times 10^{-6} C^{-2/3} Q^{1/3} w^{4/3} M^{-4/3} D^{2/3}, \quad (99)$$

which corresponds to an average dimensional heating flux per unit photospheric area:

$$\langle \mathcal{F} \rangle = (B_0^2/\mu_0) c_{A_0} F_1 \\ \langle \mathcal{F} \rangle = 1.46 \times 10^6 C^{-2/3} Q^{1/3} w^{4/3} M^{5/3} D^{1/6} \text{ ergs cm}^{-2} \text{ s}^{-1}. \quad (100)$$

This amount of flux is associated, through the turbulent cascade operating in the Kraichnan regime in the corona, with a certain characteristic turbulent velocity, v_{turb} ,¹ which we define from equation (58) to be

$$v_{\text{turb}}^2 = \int_{k_{\text{min}}}^{\infty} C \sqrt{\epsilon c_{A_0}} p^{-3/2} dp. \quad (101)$$

Using equations (64), (60), and (99), which define F_1 , this gives

$$v_{\text{turb}}^2 = (2C/\sqrt{\pi}) c_{A_0}^2 \sqrt{q F_1}; \quad (102)$$

that is, numerically,

$$v_{\text{turb}} = 70 \text{ km s}^{-1} C^{1/3} Q^{1/3} w^{1/3} M^{2/3} D^{-1/3}. \quad (103)$$

¹ The variance of the vector turbulent velocity, $\langle v^2 \rangle$, actually is $2v_{\text{turb}}^2$ and the variance of its line-of-sight component is then $2/3 v_{\text{turb}}^2$.

Adopting $C = 0.9$, as discussed in § 3, these results become more precisely:

$$\langle \mathcal{F} \rangle = 1.57 \times 10^6 Q^{1/3} w^{4/3} M^{5/3} D^{1/6} \text{ ergs cm}^{-2} \text{ s}^{-1}; \quad (104)$$

$$v_{\text{turb}} = 67 \text{ km s}^{-1} Q^{1/3} w^{1/3} M^{2/3} D^{-1/3}. \quad (105)$$

These figures are in reasonably good agreement with the observational data. A coronal loop of length 10,000 km would actually sit in the low corona, where the density could be a few 10^{10} cm^{-3} , say $2 \times 10^{10} \text{ cm}^{-3}$, while the magnetic field would be 30–50 G, giving rise to a heating flux between $2.4 \times 10^5 \text{ ergs cm}^{-2} \text{ s}^{-1}$ and $5.5 \times 10^5 \text{ ergs cm}^{-2} \text{ s}^{-1}$ for such a “quiet” region, while the line of sight rms velocity would range between 20 km s^{-1} and 27 km s^{-1} . An “active” region would have a higher density, $5 \times 10^{10} \text{ cm}^{-3}$, and a field of $\sim 100 \text{ G}$, giving rise to an heating flux of order $2 \times 10^6 \text{ ergs cm}^{-2} \text{ s}^{-1}$, and would show line of sight rms velocities of order 32 km s^{-1} .

6. DISCUSSION

The values obtained in equations (104) and (105) are in reasonable agreement with the observational data if the coronal fields are indeed in the range of a few tens of Gauss, if the density is not much less than 10^{10} cm^{-3} , and if turbulent velocities of a few tens of km s^{-1} are acceptable, which seems to be the case (Athay 1981). Figure 3 shows a more precise comparison to observational data. It presents, for $Q = 1$, and $w = 1$ ($v = 1 \text{ km s}^{-1}$), the range of magnetic field parameter M ($= B/100 \text{ G}$ and density parameter D ($= n/10^{10} \text{ cm}^{-3}$), which allow the heating flux to lie between 2×10^5 and $2 \times 10^7 \text{ ergs cm}^{-2} \text{ s}^{-1}$ with the turbulent velocities lying between 10 and 70 km s^{-1} . The shaded area in the figure indicates the region where these conditions are met, the param-

eters being also constrained to be found in a “reasonable” range of densities, $2 \times 10^9 < n < 5 \times 10^{10} \text{ cm}^{-3}$, and magnetic fields, $10 \text{ G} < B < 150 \text{ G}$.

Although we tried to define the constant C of the Kraichnan spectrum (eq. [58]) as precisely as we could, its value is still somewhat uncertain. A smaller value of C would imply larger heating rates for correspondingly smaller turbulent velocities. Conversely, if C really had a rather large value—say 10—the agreement with observational data would barely be possible, but we do not expect C to have such large values. The effects of our other simplifications to solar reality, such as assuming the turbulence to be isotropic and almost homogeneous, are expected to give rise to comparable uncertainties, since they would reflect partly in a change of coefficients of order unity ultimately multiplying C (see eqs. [57] and [58] for example).

The geometry of our model is also far from realistic yet. The main effect is probably that our translationally symmetric model for the coronal macroscopic flow underestimates the efficiency of heating, since such processes as field line tangling by large-scale flows are not represented in this description, although all the phenomena of tangling at small scales are of course incorporated in our description of the microturbulent state. The effect of a completely three-dimensional macro-

scopic motion is expected to give rise to a larger dissipation for the same level of turbulence, or conversely, to a smaller level of turbulent agitation for the same heating flux. A completely three-dimensional model certainly would be preferable to our two-dimensional one, but the step taken in § 2, which has been relatively simple here, would be intractable in most three-dimensional situations.

Of course, the idea that the corona is kept turbulent by the boundary stresses is an assumption. As explained in § 1, we believe this to be very likely true, and in fact a number of case studies support this view. Except for some slight arbitrariness left in an order-of-one dimensionless constant, our theory is otherwise parameter-free. Given the limitations of our two-dimensional model, we find it very encouraging that reasonable values of the heating flux and of the coronal microturbulent velocities are obtained from reasonable solar parameters. It should also be kept in mind that our result quantifies only that part of the heating flux which is associated with DC motions. The small-scale part of the spectrum of the photospheric motions induces coronal waves which also suffer damping and contribute a term to the heating flux that should eventually be added to the one we have calculated in this paper.

APPENDIX A

We start with equation (85) written in the form:

$$1 = \frac{\Lambda_0}{K_m} x \int_{K_m}^{K_M} K^{-5/3} \psi(x, K) dK, \quad (\text{A1})$$

where $\psi(x, K)$ is the function defined by equation (87) and in an approximate way by equation (90). Since equation (A1) is an equation for x , the various possible positions of $x^{1/2}$ and x with respect to the integration limits K_m and K_M should be discussed. Figure 4 represents, for increasing values of x the relative positions that these four different quantities may have. The third case is actually as shown, and not with the interval $(x^{1/2}, x)$, including (K_m, K_M) , because in the present case K_M is larger than K_m^2 , as is apparent from equations (93). The right-hand side of equation (A1) is then easily evaluated from equations (90a)–(90c), in all the five subcases. Let

$$I(x) = \int_{K_m}^{K_M} K^{-5/3} \psi(x, K) dK \quad (\text{A2})$$

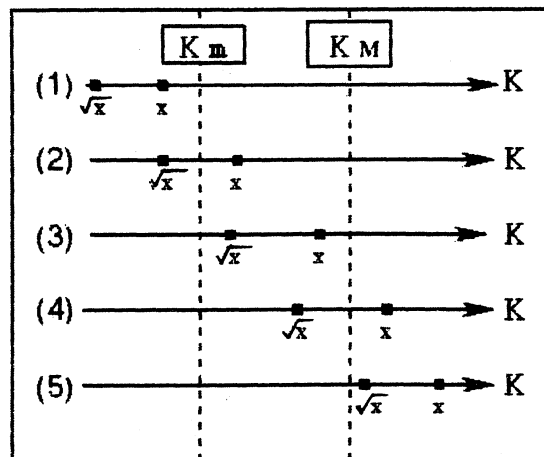


FIG. 4.—The possible relative positions of the limits of integration of the integral intervening in eq. (A1) with respect to the limits, $x^{1/2}$ and x , which define the different domains of approximation for the function $\psi(x, K)$ as defined in eqs. (89) and (90) of the main text.

Then we have

$$\begin{aligned} \text{subcase 1: } I(x) &= \int_{K_m}^{K_M} K^{-2/3} dK ; \\ \text{subcase 2: } I(x) &= \int_{K_m}^x xK^{-5/3} dK + \int_x^{K_M} K^{-2/3} dK ; \\ \text{subcase 3: } I(x) &= \int_{K_m}^{\sqrt{x}} x^2K^{-11/3} dK + \int_{\sqrt{x}}^x xK^{-5/3} dK + \int_x^{K_M} K^{-2/3} dK ; \\ \text{subcase 4: } I(x) &= \int_{K_m}^{\sqrt{x}} x^2K^{-11/3} dK + \int_{\sqrt{x}}^{K_M} xK^{-5/3} dK ; \\ \text{subcase 5: } I(x) &= \int_{K_m}^{K_M} x^2K^{-11/3} dK . \end{aligned}$$

From this we obtain five forms of the equation (A1), each valid in one of the subintervals of the x -axis corresponding to these five subcases, which are

$$\begin{aligned} \text{subinterval 1: } & x < K_m ; \\ \text{subinterval 2: } & K_m < x < K_m^2 ; \\ \text{subinterval 3: } & K_m^2 < x < K_M ; \\ \text{subinterval 4: } & K_M < x < K_M^2 ; \\ \text{subinterval 5: } & K_m^2 < x \end{aligned}$$

These forms are the following:

$$\begin{aligned} \text{subinterval 1: } & 1 = \frac{3\Lambda_0}{K_m} x(K_M^{1/3} - K_m^{1/3}) ; \\ \text{subinterval 2: } & 1 = \frac{3\Lambda_0}{K_m} \left(\frac{x^2}{2} K_m^{-2/3} - \frac{3}{2} x^{4/3} + xK_M^{1/3} \right) ; \\ \text{subinterval 3: } & 1 = \frac{3\Lambda_0}{K_m} \left(\frac{x^3}{8} K_m^{-8/3} + \frac{3}{8} x^{5/3} - \frac{3}{2} x^{4/3} + xK_M^{1/3} \right) ; \\ \text{subinterval 4: } & 1 = \frac{3\Lambda_0}{K_m} \left(\frac{x^3}{8} K_m^{-8/3} + \frac{3}{8} x^{5/3} - \frac{1}{2} x^2 K_M^{-2/3} \right) ; \\ \text{subinterval 5: } & 1 = \frac{3\Lambda_0}{K_m} (K_m^{-8/3} - K_M^{-8/3}) \frac{x^3}{8} . \end{aligned}$$

The various right-hand sides of these equations constitute a continuous and continuously differentiable approximation to the function on the right-hand side of equation (A1).

REFERENCES

- Athay, G. 1981, in *The Sun as a Star*, ed. S. Jordan (NASA SP 450), 85
 Athay, G., & White, S. 1979, *ApJ*, 226, 1135
 Bondeson, S. 1985, *Phys. Fluids*, 28, 2406
 Browning, P., & Priest, E. R. 1984, *A&A*, 131, 283
 Chiuderi, C. 1980, in *Solar Phenomena in Stars*, NATO ASI Ser., ed. R. M. Bonnet & A. K. Dupree (Dordrecht: Reidel) 129
 Chiueh, T., & Zweibel, E. 1987, *ApJ*, 317, 900
 Grappin, R., Frisch, U., Léorat, J., & Pouquet, A. 1982, *A&A*, 105, 60
 Grossmann, W., & Smith, R. A. 1988, *ApJ*, 332, 476
 Hasegawa, H., & Uberoi, C. 1982, *The Alfvén Wave* (Washington, DC: Tech Inform. Ctr., US DOE)
 Heyvaerts, J. 1990, *IAU Symp. 142, Basic Plasma Processes in the Sun*, ed. V. Krishan & E. R. Priest (Dordrecht: Kluwer), 207
 Heyvaerts, J., & Priest, E. R. 1983, *A&A*, 117, 270
 ———. 1984, *A&A*, 137, 63
 Hollweg, J. V. 1984, *ApJ*, 277, 392
 Ionson, J. A. 1982, *ApJ*, 254, 318
 Kraichnan, R. H. 1965, *Phys. Fluids*, 8, 138
 Kuperus, M., Ionson, J. A., & Spicer, D. 1981, *ARA&A*, 19, 7
 Malherbe, J. M., Mein, P., Müller, R., Roudier, T., Coutard, C., & Hellier, R. 1987, *Proc. Soho-Themis Workshop, Paris*, ed. P. Lemaire & Z. Mouradian (Paris: Observ. de Paris), 53
 Mein, N., & Schmieder, B. 1981, *A&A*, 97, 310
 Montgomery, D. 1990, *IAU Symp. 142, Basic Plasma Processes in the Sun*, ed. V. Krishnan & E. R. Priest (Dordrecht: Kluwer), 215
 Montgomery, D., Phillips, L., & Theobald, M. L. 1989, *Phys. Rev. A*, 40, 1515
 Parker, E. N. 1983, *ApJ*, 264, 642
 Pettini, M., Nocera, L., & Vulpiani, A. 1985, in 'Chaos in Astrophysics', ed. J. R. Butler (Dordrecht: Reidel), 305
 Poedts, S., Goossens, M., & Kerner, W. 1990, *Solar Phys.*, in press
 Pouquet, A., Frisch, U., & Léorat, J. 1976, *J. Fluid Mech.*, 77, 321
 Roudier, T., Mein, P., Müller, R., Vigneau, J., Malherbe, J. M., & Espagnet, O. 1990, *A&A*, submitted
 Roudier, T., & Müller, R. 1987, *Solar Phys.*, 107, 11
 Schatzman, E. 1949, *Ann. d'Ap.*, 12, 203
 Strauss, R. 1986, *Phys. Fluids*, 29, 3668
 Taylor, J. B. 1986, *Rev. Mod. Phys.*, 58, 741
 Ting, A., Matthaeus, W., & Montgomery, D. 1986, *Phys. Fluids*, 29, 3261
 Tsinganos, K. C., Distler, J., & Rosner, R. 1984, *ApJ*, 278, 409
 Vaiana, G., & Rosner, R. 1978, *ARA&A*, 16, 393
 van Ballegooijen, A. A. 1986, *ApJ*, 311, 1001
 ———. 1990, *IAU Symp. 142, Basic Plasma Processes in the Sun*, ed. V. Krishnan & E. R. Priest (Dordrecht: Kluwer), 303
 Vekstein, V. 1987, *A&A*, 182, 324
 Wentzel, D. 1979, *ApJ*, 227, 319